ISSN 1392–1207. MECHANIKA. 2020 Volume 26(4): 301–310

Research on Vehicle-Bridge Vertical Coupling Dynamics of Monorail based on Multiple Road Excitations

Zhouzhou XU*, Zixue DU, Zhen YANG***, Junchao ZHOU******
**Chongqing Jiaotong University, Chongqing, 400074 China, E-mail: xuzhouzhou@hotmail.com*
***Chongqing Jiaotong University, Chongqing, 400074 China, E-mail: aaad@163.com*
****Chongqing Jiaotong University, Chongqing, 400074 China, E-mail: 21930315@qq.com*
*****Chongqing Jiao tong University, Chong Qing 400074, China, E-mail: zhou1987g@163.com*
School of Mechanical Engineering, Sichuan University of Science and Engineering, Zigong, Sichuan ,643000, China

crossref http://dx.doi.org/10.5755/j01.mech.26.4.24399

1. Introduction

With the development of social economy, traffic congestion has become one of the most serious problems in cities. The whole world is committed to solving the traffic congestion. Bus and urban rail transit are their solutions, especially urban rail transit, which play an obvious role in solving the problem of traffic congestion [1]. Compared with metro, straddle monorail has the advantages of low cost, small turning radius, strong climbing ability and low vibration and noise. Its successful application in Chongqing has attracted more attention [2].

Vehicle-bridge coupling dynamics of railway vehicles is the basis of vehicle vibration and noise, fatigue life of vehicle body, fatigue of track beam structure, etc. [3]. Its output is the input condition for all body and track problems. However, due to the wide use and history of monorail far behind Metro vehicles, there are few studies on Vehicle-bridge Coupling Dynamics of monorail, and the accuracy and depth of some results are not satisfactory.

The monorail vehicles use rubber tyres, and track mostly uses pre-stressed reinforced concrete beams (PC beam). A unique bogie structure is used between the car body and tires to transfer forces in all directions. The wheel-rail coupling relationship is obviously different from that of metro vehicles and ordinary vehicles, so the wheel-rail coupling dynamics of other vehicles is not suitable for monorail trains [2].

There are some studies on straddle-type monorail transportation, but the number is small and not enough in-depth, that is, first, there is no complete train-bridge coupling dynamic model; second, there is a single road excitation, which is far from the actual situation; finally, there is a lack of experimental data to verify the correctness.

Du Zixue, a professor of Chongqing Jiaotong University, has studied monorail for many years, a set of theoretical and experimental system including vehicle, track and operation management is formed, and the road incentive is roughness [4-10].

Naeimi et al. used finite element method and dynamic simulation to study the deformation of track beam under compression, the coupling dynamic response of vehicle-bridge under the condition of elastic beam is calculated, and the correctness of the model is verified by comparing the dynamic simulation results of tires with those of vehicle manufacturers [11]; Lv, KK et al. studied the influence of wheel eccentricity on the vertical vibration of the suspended monorail vehicle through experiments and simulations, and determined that the abnormal vibration of the body was mainly caused by the wheel eccentricity [12]; Kim. CW et al. studied the dynamic response of steel beams under strong earthquakes with consideration of vehicle-bridge interaction, and the aseismic behavior of monorail rail beam with steel structure is affirmed [13].

Pu, QH et al. have studied the fatigue performance of PC beams in straddle monorail system, carried out stiffness degradation and strain change tests, tested the displacement and rotation of concrete beams and steel bars, and established a three-dimensional finite element model [14]. Gou et al. have studied the dynamic characteristics of bridges under load by finite element method, and then, based on the simulation results, the influencing factors of bridges and evaluated the ride comfort of trains has been studied [15].

Based on the theory of vehicle-bridge coupled vibration, Bao et al. studied the influence of track irregularity on the operation of suspended monorail by using finite element method and dynamic method [16].

2. Dynamic model

2.1. Monorail train model

This paper is based on the Chongqing Railway Line 3. The train consists of several cars, including one head car, one tail car and four to six middle cars. Each car consists of two bogies and one body. The structure of the head car and the tail car is the same, which with one power bogie and one non-power bogie, and the middle car has two power bogies. The cars are connected by couplers, and the force transfer part of coupler is composed of rubber. Only the longitudinal force is transmitted, and the axial torsional stiffness is very small. Because the dynamics of the mid-train is the same, the four-body train dynamics model is adopted in this paper as it shows in Fig. 1, and the key dynamic parameters are shown in Table 1.

2.2. The body subsystem

Ignoring the influence of electrical equipment on the mass distribution and vibration of the car body, the car body is regarded as a rigid body, and the model has the same shape parameters and dynamic parameters as the actual car body.

Vertical force is transmitted between car body and bogie by air spring, and longitudinal force is transmitted by

center pin. Spring force is transmitted between front car and rear car by coupler, as shown in Fig. 2.

M represent the mass and *I* represent the moment of inertia, *X*, *Y* and *Z* represent the three coordinates of the Cartesian coordinate system, and subscripts 1, 2 and 3 represent the head car, the second car and the third car respectively; αrepresents the turning angle of the part around the coordinate axis, and subscripts x, y and z represent the *X*, *Y* and *Z* axes; *K* and *C* represent the stiffness and damping of the air spring; subscripts *v* and *t* represent the vertical and horizontal; K_p is the radial stiffness of the coupler, and *F* is the arm of the coupler pulling force relative to the body center of the body. F_f and F_r represent the longitudinal force of the front and rear car to the body, and T_f and T_r represent the moment of the front and rear car to the body around the y-axis; Subscript c marks the body, Subscript *z* marks the bogie; Each car has two bogies, with the subscript *f* and *r* mark the front and rear bogies. The dynamic equation of the train body is as follows:

$$
\begin{cases}
\mathrm{M}_c \ddot{Z}_c = (-4Z_c + 2\Delta Z_{z1} + 2\Delta Z_{z2})K_c + (-4\dot{Z}_c + 2\dot{Z}_{z1} + 2\dot{Z}_{z2})C_c \\
\mathrm{M}_c \ddot{Y}_c = (-2Y_c + \Delta Y_{z1} + \Delta Y_{z2})K_q + (-2\dot{Y}_c + \dot{Y}_{z1} + \dot{Y}_{z2})C_q \\
\mathrm{M}_c \ddot{X}_c = (-2X_c + \Delta X_{z1} + \Delta X_{z2})K_q + (-2\dot{X}_c + \dot{X}_{z1} + \dot{X}_{z2})C_q + F_f + F_r + M_c g \cdot \alpha_y \\
F_f = (\Delta X_{c2} - \Delta X_{c1})K_T \\
F_r = (\Delta X_{c3} - \Delta X_{c2})K_T \\
\mathrm{I}_{cx} \ddot{\alpha}_x = -[(4\alpha_x - 2\beta_{x1} - 2\beta_{x2})K_c - (4\dot{\alpha}_x - 2\dot{\beta}_{x1} - 2\dot{\beta}_{x2})C_c]C^2 \\
\mathrm{I}_{cy} \ddot{\alpha}_y = (-4\alpha_y l - 2\Delta Z_{z1} + 2\Delta Z_{z2})lK_c - (4\dot{\alpha}_y l + 2\dot{Z}_{z1} - 2\dot{Z}_{z2})lC_c + \mathrm{T}_f + \mathrm{T}_r \\
\mathrm{I}_{cz} \ddot{\alpha}_z = [-(2\alpha_y l - \Delta Z_{z1} + \Delta Z_{z2})K_q - (2\dot{\alpha}_y l - \dot{Z}_{z1} + \dot{Z}_{z2})C_q]l \\
T_f = (\Delta X_{c2} - \Delta X_{c1})K_T \bullet f \\
T_r = (\Delta X_{c3} - \Delta X_{c2})K_T \bullet f
\end{cases}
\tag{1}
$$

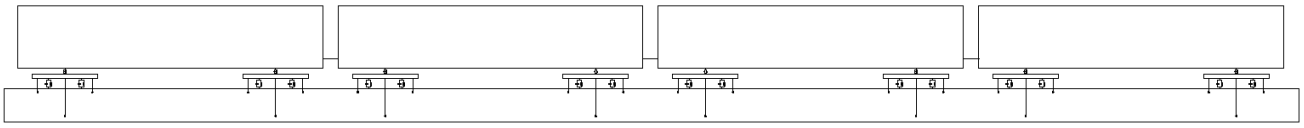

Fig. 1 The dynamics model of the monorail train

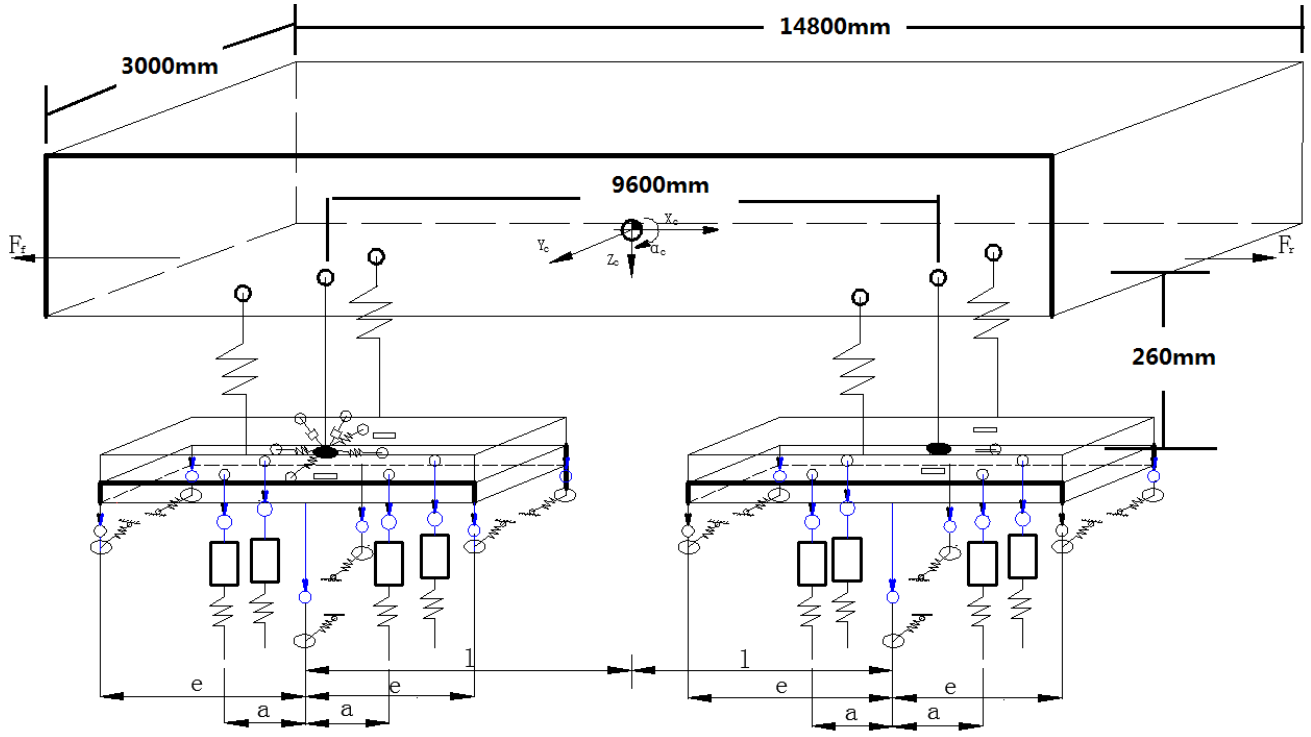

Fig. 2 Dynamics principle diagram of the Body and Bogie

Table 1

Car dynamics parameters

Project	Value	Project	Value
Body mass in AW3, kg	25800	running wheel mass, kg	54
Bogie mass, kg	5600	Guide wheel mass, kg	30
Rotational Inertia of Body Ixx, kg•m^2	43000	Vertical stiffness of running wheel, N/m	1200000
Rotational Inertia of Body Iyy, kg•m^2	365000	Vertical Damping of Traveling Wheel, N•s/m	3400
Rotational Inertia of Body Izz, kg•m^2	365000	Radial stiffness of guide wheel, N/m	980000
Rotational Inertia of Bogie Ixx, kg•m^2	2400	Radial Damping of Guide Wheel, N•s/m	3120
Rotational Inertia of Bogie Iyy, kg•m^2	3400	Vertical stiffness of air spring, N/m	160000
Rotational Inertia of Bogie Izz, kg•m^2	9600	Longitudinal stiffness of traction rubber stack, N/m	490000

The matrix form is:

$$\overrightarrow{M_c} \times \overrightarrow{a_c} = \overrightarrow{\Delta X_c} \times \overrightarrow{K_c} + \overrightarrow{v_c} \times \overrightarrow{C_c} + \overrightarrow{F_{fc}} + \overrightarrow{F_{rc}} + \overrightarrow{F_{Gc}}, \tag{2}$$

here: $\overrightarrow{M}$ is the inertia matrix; $\vec{a}$ is the acceleration matrix; $\overrightarrow{\Delta X}$ is the distance matrix; $\overrightarrow{K}$ is the stiffness matrix, impact of the front car; $\overrightarrow{F_r}$ is the impact of the rear car; $\overrightarrow{F_G}$ is the impact of gravity.

From Eqs. (1) and (2), the body model of Adams is established, as shown in Fig.3.

Ignoring the influence of electrical equipment on the mass distribution and vibration on the body, the body is regarded as a rigid body, and make the model have the same shape parameters and dynamic parameters as the actual body.

The left and right air springs are used to transfer the vertical force between each bogie and the body, the transverse stiffness and the longitudinal stiffness of the air spring are the same, and the vertical and transverse stiffness-damp spring model is used to simulate the air spring.

The center pin is used to transfer tractive force and braking force between bogie and body, rubber piles are arranged between the center pin and body to reduce shock, and it is simulated by the contact force between the center point of the center pin and the body parts.

2.3 The bogie subsystem

As the front Bogie and the rear bogie have the same force condition, as shown in Fig. 2, they have the same dynamic equation. For the former bogies, as an example (subscript 1), *K* and *C* are the equivalent stiffness and damping of tires, subscript *z* is the running wheel, subscript *d* is the guiding wheel and the stabilizing wheel (the guiding wheel and the stabilizing wheel are the same), subscript *h* is the lateral direction of tires. The front bogie is taken as an example in Eqs. (3) and (4). Eqs. (3) is the matrix form of Eqs. (4).

$$\left.\begin{aligned}
&M_{z1}\ddot{Z}_{z1} = 2(\Delta Z_c + \alpha_y l - \Delta Z_{z1})K_c + 2(\dot{Z}_c + \dot{\alpha}_y l - \dot{Z}_{z1})C_c - \\
&\qquad 4\Delta Z_{z1}K_z - 4\dot{Z}_{z1}C_z - 6\Delta Z_{z1}K_{dh} - 6\dot{Z}_{z1}C_{dh} \\
&M_{z1}\ddot{Y}_{z1} = (\Delta Y_c - Y_{z1})K_R + (\dot{Y}_c - \dot{Y}_{z1})C_R - 6\Delta Y_{z1}K_d \\
&M_{z1}\ddot{X}_{z1} = (X_c - \Delta X_{z1})K_c + f_q + M_{z1}g\cdot\beta_{y1} \\
&I_{zx}\ddot{\beta}_{x1} = 2(\alpha_x - \beta_{x1})K_c c^2 + 2(\dot{\alpha}_x - \dot{\beta}_{x1})C_c c^2 + (-4\beta_{x1}h_d{}^2 - 2\beta_{x1}h_w{}^2)K_d + \\
&\qquad (-4\dot{\beta}_{x1}h_d{}^2 - 2\dot{\beta}_{x1}h_w{}^2)C_d - 4\beta_{x1}K_z b^2 - 4\dot{\beta}_{x1}C_z b^2 - 6\beta_{x1}K_{dh}w^2 - 6\dot{\beta}_{x1}C_{dh}w^2 \\
&I_{zy}\ddot{\beta}_{y1} = -4\beta_{y1}K_z b^2 - 4\dot{\beta}_{y1}C_z b^2 - 4\beta_{y1}K_{dh}e^2 - 4\dot{\beta}_{y1}C_{dh}e^2 \\
&I_{zz}\ddot{\beta}_{z1} = -4\beta_{z1}K_d e^2 - 4\dot{\beta}_{z1}C_d e^2
\end{aligned}\right\}. \tag{3}$$

$$\overrightarrow{M_{z1}} \times \overrightarrow{a_{z1}} = \overrightarrow{\Delta X_{z1}} \times \overrightarrow{K_{z1}} + \overrightarrow{v_{z1}} \times \overrightarrow{C_{z1}} + \overrightarrow{F_{Gz1}} + \overrightarrow{F_q}, \tag{4}$$

here: $\overrightarrow{M_{z1}}$ is the inertia matrix; $\overrightarrow{a_{z1}}$ is the acceleration matrix; $\overrightarrow{\Delta X_{z1}}$ is the distance matrix; $\overrightarrow{K_{z1}}$ is the stiffness matrix; $\overrightarrow{v_{z1}}$ is the velocity matrix; $\overrightarrow{C_{z1}}$ is the damping matrix and $\overrightarrow{F_{Gz1}}$ is the impact of gravity; $\overrightarrow{F_q}$ is the driving force influence.

From Eqs. (3) and (4), the bogie model of Adams is established, as shown in Fig. 3.

As this paper mainly studies the vertical dynamics of vehicles, to simplify the calculation, the frame structure (rigid body) is used, ignoring the internal structural and external characteristics of the bogie, and ensure that the frame and the original bogie have the same mass, roughly shape size, centroid position, moment of inertia, force point position.

The straddle-type monorail vehicles use rubber tires. Each bogie has four running wheels, four guiding wheels and two stabilizing wheels. The guiding wheels and stabilizing wheels are the same. Both guiding wheels and stabilizing wheels are prestressed by 5000 N. The running wheels are special tires. Based on the dynamic stiffness and damping of the two tires measured by tire test, a tire model is established by using Ftire model (Fig. 3).

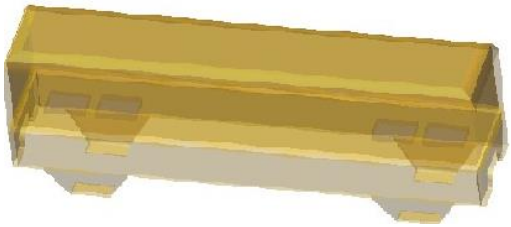

a) the model Body

a) the model of Bogie

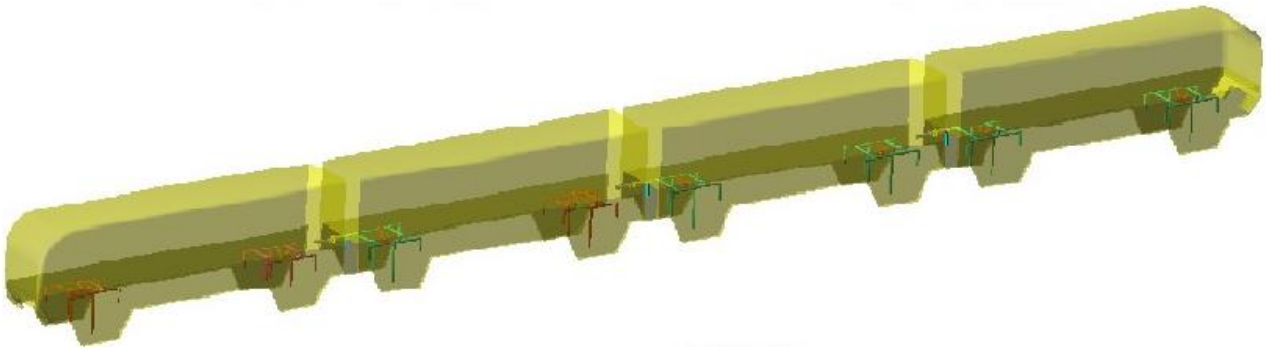

b) the model of the train

Fig. 3 Adams model of the Body and Bogie

2.4. Rail line model

Chongqing Railway Line 3 adopts the line system of PC beam and steel beam, in which steel beam is mainly used in track bridge and turnout system, and most of the track beams are PC beams. The calculation in this paper is only for PC beams, only considering the straight line section and ignoring the construction error.

Typical PC Straight Beams are all 22000mm long, 850mm wide and 1500mm high, there are 40 steel bars in the longitudinal arrangement. The track beams are connected by finger bands. As PC beams are manufactured by Compression Molding and have good surface smoothness, so the input of road roughness is defined as Class A (Fig.4).

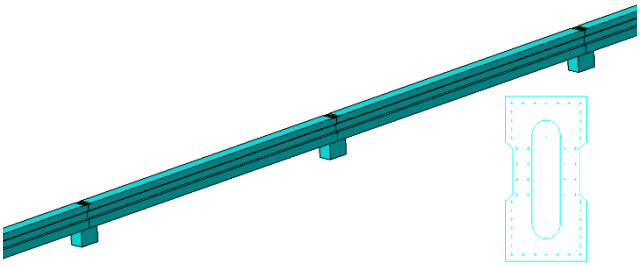

Fig. 4 Track model

Traditionally, two methods are commonly used to deal with track beams: road model with road spectrum or beams with certain stiffness and damping. The former ignores the influence of compression deformation of PC beams on trains, while the latter ignores the influence of road spectrum on trains. In this paper, road elasticity is proposed to solve this problem. Processing Monorail Lines into Roads, and the grade of road roughness is Class A. The load spectrum is used to simulate the deformation of the track beam caused by pressure(DTP): applying moving surface contact force on track beam in Abaqus to simulate the operation of monorail train on track, then the DTP is transformed into the load spectrum and applied to the axles of the train in Adams. The motion of axles is calculated. Then the calculated results are converted into loads and input into Abaqus. Finally, the vertical force converted from the DTP calculated after three iterations is used as the input of the axle in Adams (Figs. 5, 6 and Eq. (5)). Among them, ΔZ_b is the deformation of the track beam calculated by Abaqus, F_x is the dynamic force on the axle equivalent to ΔZ_b in Adams, F_p is the axle simulation force applied on the track beam in Abaqus, g is the gravity acceleration, and ΔZ_a is the vertical relative displacement of the axle.

When a running tire passes through the finger band (Fig. 7), the uneven pressure on the ground of the tire changes its deformation and causes the tire to vibrate vertically. This paper simulates the influence of the finger plate on the train operation by applying the equivalent force (load spectrum) on the running wheel axle [17].

$$\begin{cases} F_x = -2\Delta Z_b \times K_z \\ F_p = \frac{1}{4} m_c \times g + \frac{1}{2} \ddot{Z}_a m_Z + (\Delta Z_c + \alpha_y l - \Delta Z_{z1}) K_c + (\dot{Z}_c + \dot{\alpha}_y l - \dot{Z}_{z1}) C_c \end{cases} \quad (5)$$

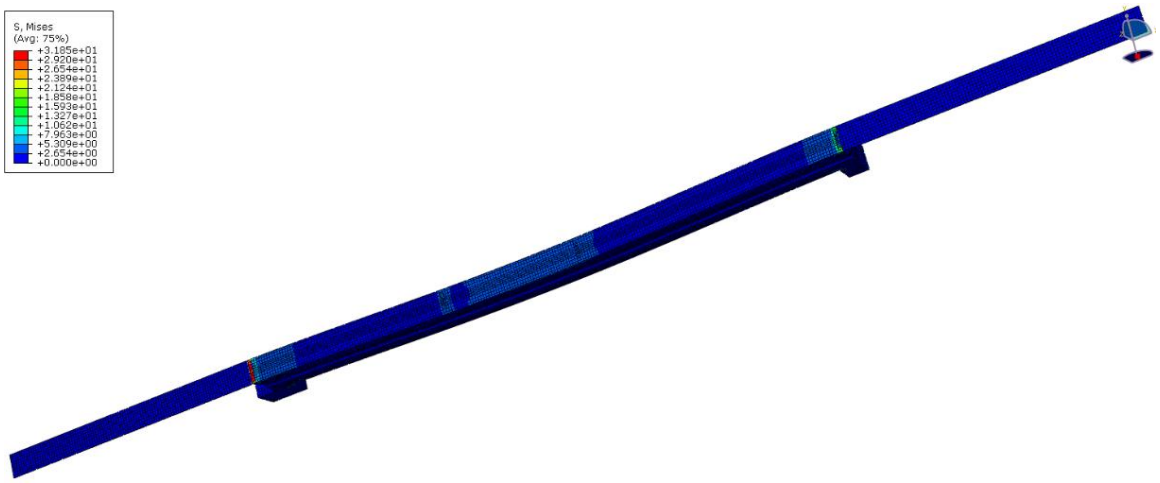

Fig. 5 Stress nephogram of track beam at different locations of train

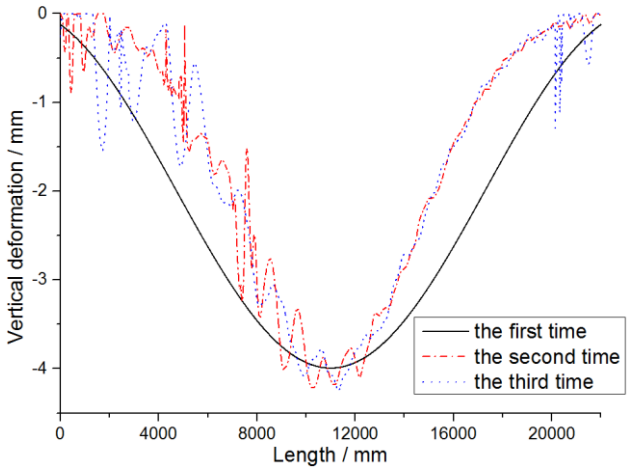

Fig. 6 The results of three times

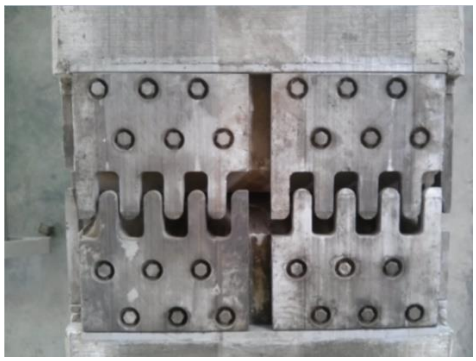

a) The finger band

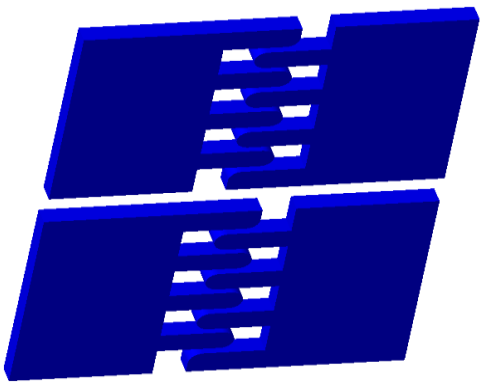

b) The model of finger band

Fig. 7 Finger band

2.5. Vertical dynamics modelling of monorail train

The gravity mode is set up, and the built train model is imported in ADAMS. According to the dynamic principle, the DTP and the influence of finger plate are equivalent to the vertical force on the running wheel axle. As this paper only deals with the straight-line working condition, three pavements in the position of running wheel and guiding wheel respectively are established. The length of the roads is 150 meters and the roughness of the road is Class A. The train is directly placed on the track beam according to the geometric size, and the guide wheels and the stabilizer wheels are pre-stressed by 5000 N.

3. Coupled dynamic simulation of vehicle-bridge system

Using the established train model, dynamic simulation is carried out in ADAMS. The train speed is set to 43 km/h, the track length is set to 150 meters (composed of track beam and finger plate), and the simulation time is set to 12 seconds. This paper focuses on the influence of vertical excitation on trains, so linear track is adopted, and only vertical effect is considered in simulation data comparison. In ADAMS modelling, the vehicle is placed on the track according to the geometric size, without considering the tire deformation, there will be a vertical vibration at the beginning of the simulation, so the first two seconds of simulation data are ignored.

4. Experiments and contrasts

From 1:00 to 5:00 a.m. on October 27, 2017, a train test was conducted at Tongyuan Bureau to Longtousi Section of Chongqing Railway Line 3. The vehicle was loaded with counterweight to simulate AW3 working conditions, and the vibration acceleration of various points of the middle car was measured (Fig. 8, Table 2). The sampling frequency of the accelerometer used in the experiment is 2000 Hz, and a relatively straight section of the line is selected for comparison. The travel distance is 100 s.

As body center and the bogie of the car can better reflect the vertical vibration characteristics in the process of train operation, this paper selects the data of the body centers, the first bogie and the first axle of the first bogie for comparison, and adopts the simulation data of time-domain signals (Figs. 9-11) and frequency domain signal (Fig. 12).

a) The tset train

b) The sensor on the bogie c) The sensor on the car

Fig. 8 The test of the train

4.1. Time domain analysis

The DTP has an obvious influence on the vertical vibration of the vehicle in time domain. The simulation data show that the amplitude of the whole car body is very small without the influence of track beam deformation, but the vibration amplitude of the train is obvious when passing through the finger plate, and the simulation data are quite different from the measured data. The vertical vibration amplitude has been significantly improved after adding the DTP, the simulation data are close to the measured values. It can be seen that the influence of DTP on the vertical vibration of the train is much greater than that of the road roughness. The simulation results are close to the measured values when the DTP added, but the vibration is still nearly 20% smaller than the measured values, because the ideal straight line is used in the simulation, while the actual line height and turning conditions are ignored (Figs. 9-11).

Table 2

Sensor channel

No.	coor-dinate	direction	position	sampling frequency	Sensitivity coeffi-cient, mv/g
1	*x*	longitudinal	The first axle of the first bogie of the second car	2000	-20
2	*y*	lateral	The first axle of the first bogie of the second car	2000	20
3	*z*	vertical	The first axle of the first bogie of the second car	2000	-20
4	*x*	longitudinal	The second axle of the first bogie of the second car	2000	-20
5	*y*	lateral	The second axle of the first bogie of the second car	2000	20
6	*z*	vertical	The second axle of the first bogie of the second car	2000	-20
7	*x*	longitudinal	The Frame Center of the first bogie of the second car	2000	100
8	*y*	lateral	The Frame Center of the first bogie of the second car	2000	100
9	*z*	vertical	The Frame Center of the first bogie of the second car	2000	-100
10	*x*	longitudinal	The left air spring seat of the first bogie of the second car	2000	100
11	*y*	lateral	The left air spring seat of the first bogie of the second car	2000	100
12	*z*	vertical	The left air spring seat of the first bogie of the second car	2000	-100
13	*x*	longitudinal	The right air spring seat of the first bogie of the second car	2000	100
14	*y*	lateral	The right air spring seat of the first bogie of the second car	2000	100
15	*z*	vertical	The right air spring seat of the first bogie of the second car	2000	-100
16	*x*	longitudinal	The first axle of the second bogie of the second car	2000	-20
17	*y*	lateral	The first axle of the second bogie of the second car	2000	20
18	*z*	vertical	The first axle of the second bogie of the second car	2000	-20
19	*x*	longitudinal	The second axle of the second bogie of the second car	2000	-20
20	*y*	lateral	The second axle of the second bogie of the second car	2000	20
21	*z*	vertical	The second axle of the second bogie of the second car	2000	-20
22	*x*	longitudinal	The Frame Center of the second bogie of the second car	2000	100
23	*y*	lateral	The Frame Center of the second bogie of the second car	2000	100
24	*z*	vertical	The Frame Center of the second bogie of the second car	2000	-100
31	*x*	longitudinal	Mid-floor of the second car	2000	100
32	*y*	lateral	Mid-floor of the second car	2000	100
33	*z*	vertical	Mid-floor of the second car	2000	-100
34	*x*	longitudinal	Front floor of the second car	2000	100
35	*y*	lateral	Front floor of the second car	2000	100
36	*z*	vertical	Front floor of the second car	2000	-100
37	*x*	longitudinal	Rear floor of the second car	2000	100
38	*y*	lateral	Rear floor of the second car	2000	100
39	*z*	vertical	Rear floor of the second car	2000	-100

4.2. Spectrum analysis

FFT is applied to the three groups of vertical vibration values of the first bogie center. Compared with before adding DTP, the vibration frequency of the bogie center is similar after adding the DT, but the main frequency of vibration changes from 4.4 Hz to 3.4 Hz, the corresponding amplitude of the main frequency decreases from 0.45 m/s^2 to 0.26 m/s^2, and the corresponding bandwidth of the main frequency decreases from 0.3 Hz to 0.16 Hz. The measured data show that the main frequency of the vibration is 3.7 Hz,

the corresponding amplitude of the main frequency is 0.18 m/s^2, and the corresponding bandwidth is 0.14 Hz. It can be seen that the simulation data are closer to reality by adding the DTP. The simulation data have corresponding amplitudes near 4.4 Hz and 5. 9 Hz, which are close to the measured ones. After 10 Hz, the central amplitude of the front bogie is almost zero (Fig. 12).

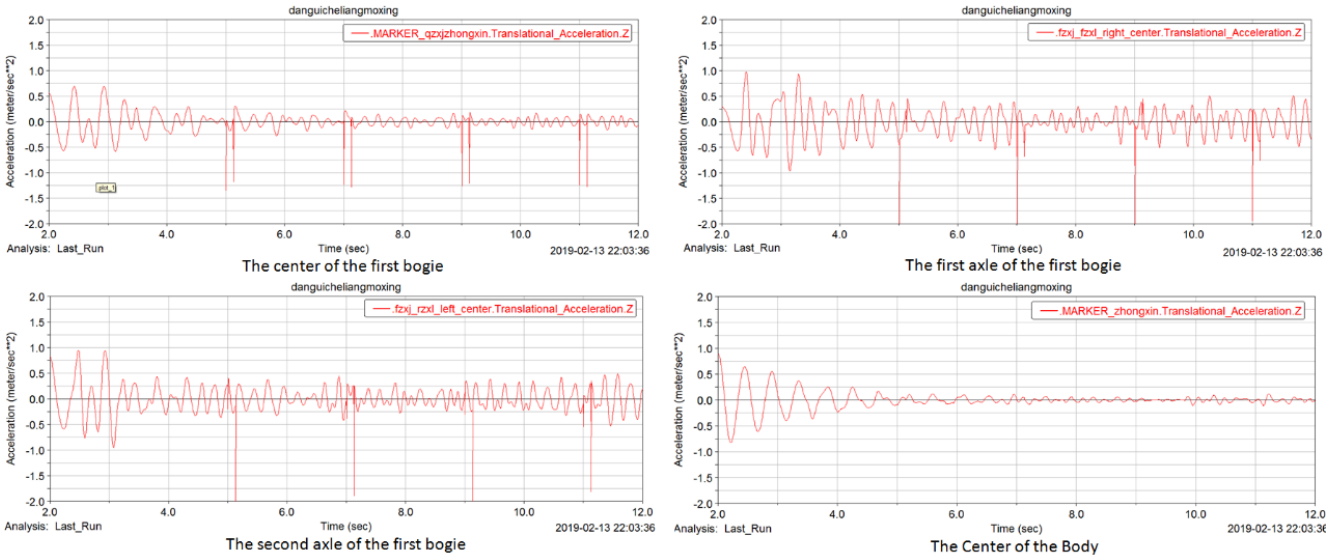

Fig. 9 Simulation time-domain diagram before adding the DTP (vertical acceleration)

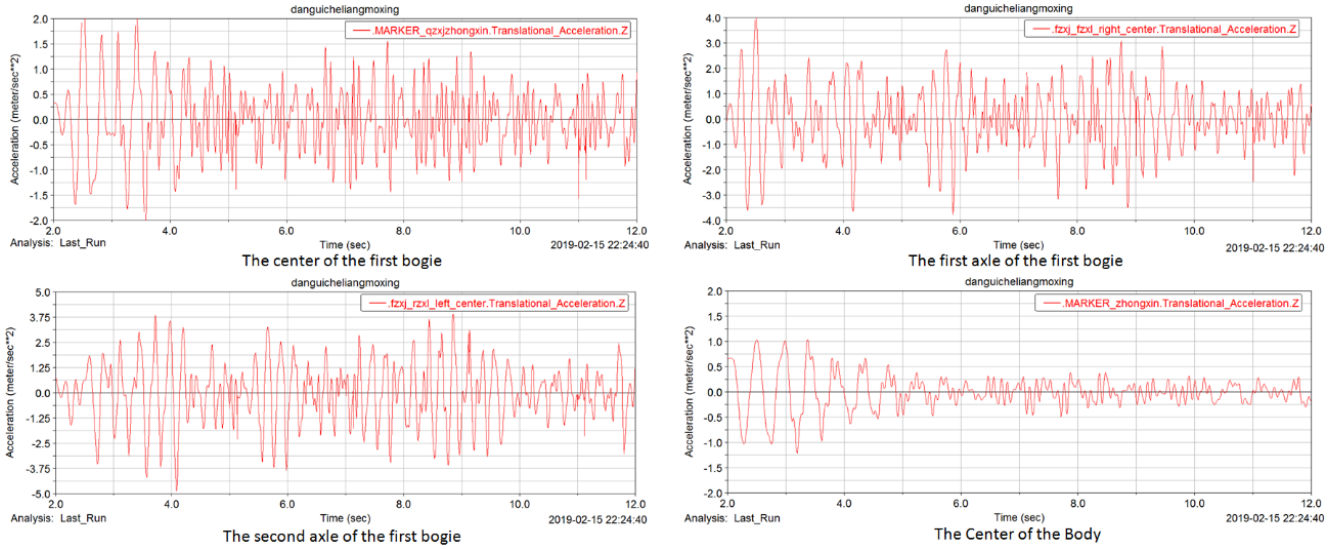

Fig. 10 Simulation time-domain diagram after adding the DTP (vertical acceleration)

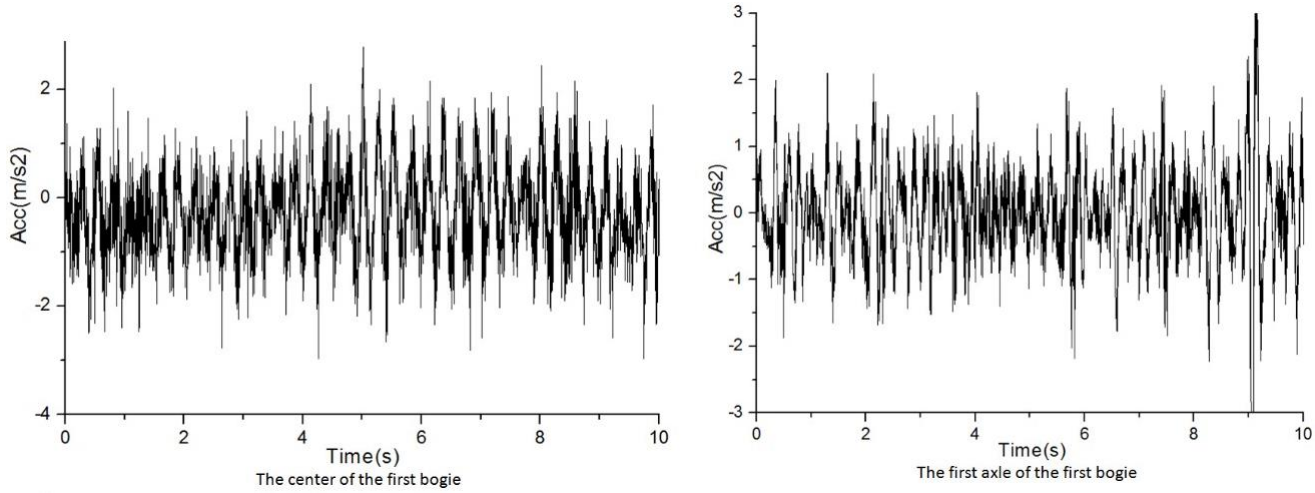

Fig. 11 Measured values (vertical acceleration) 2

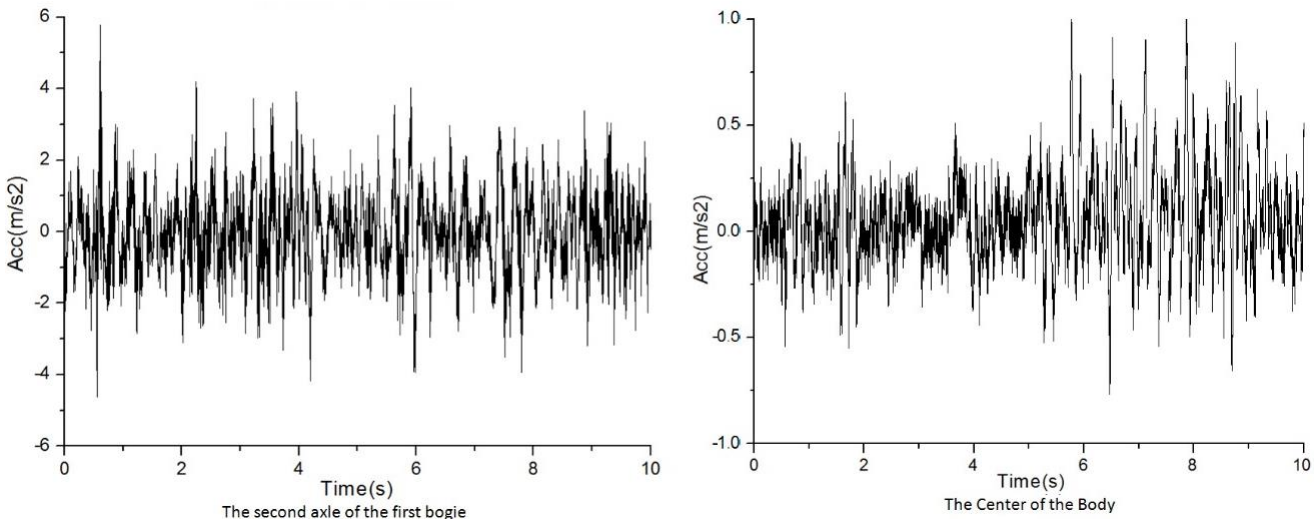

Fig. 11 Continuation

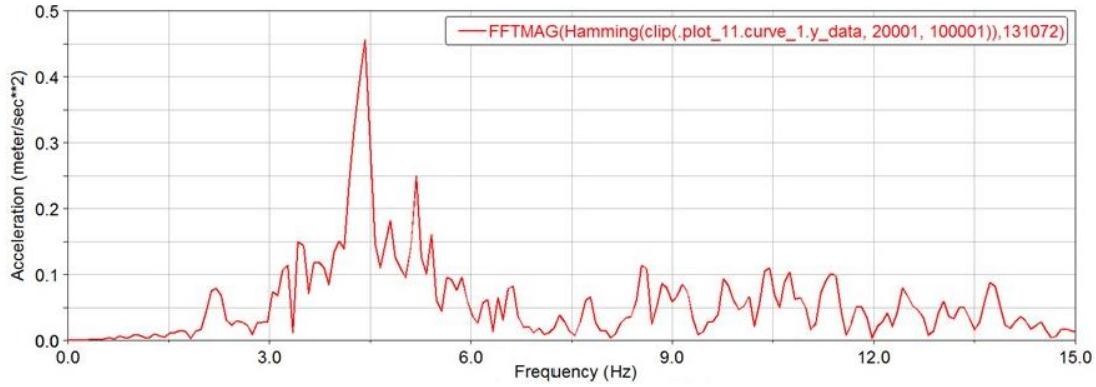

a) Simulation data before DTP added

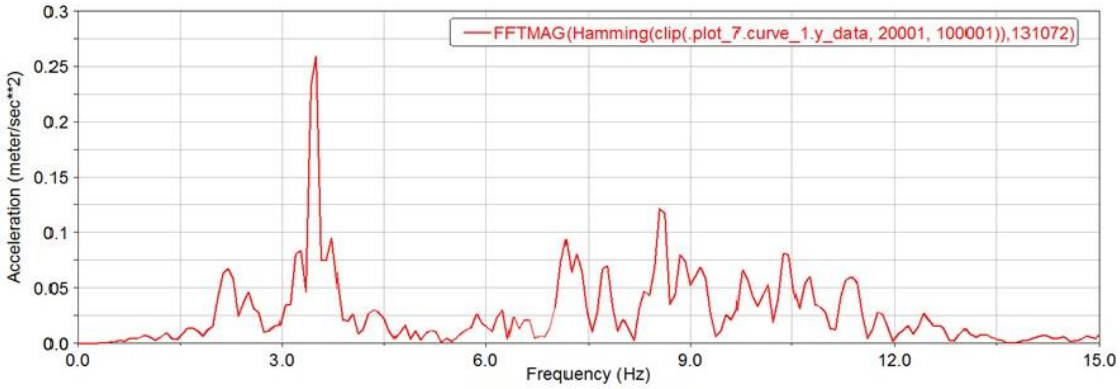

b) Simulation data after DTP added

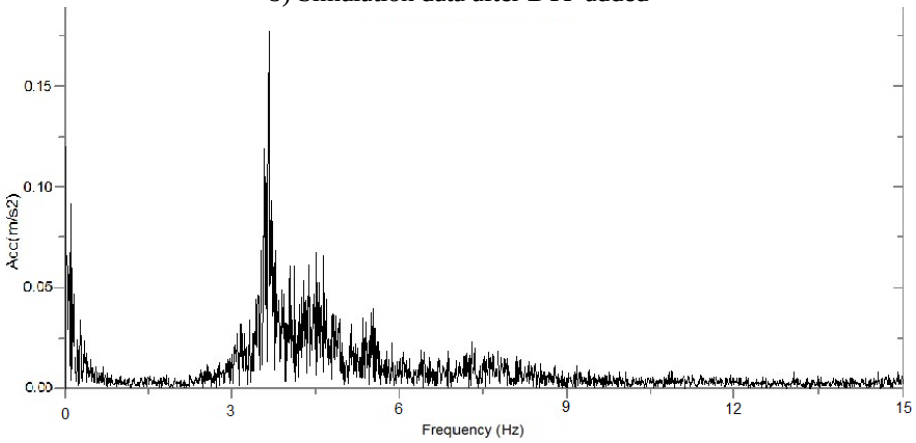

b) Experimental data

Fig. 12 FFT Transform value of vertical acceleration of the first Bogie center

5. Conclusion

In order to study the vertical dynamic effect of straddle monorail train, the train dynamic model and simulation model with coupler are established. The finite element model of PC beam is established and the vertical deformation of PC beam is simulated under moving load, the results are converted into load spectrum and applied on the axle, then the simulation results of vehicle dynamics are taken as moving loads, and the deformation of PC beam is calculated again in the finite element software, finally, the vertical force converted from the dynamic deformation of track beam calculated after three iterations is used as the input of axle in Adams. The effect of finger plate on the vertical motion of train is simplified to load spectrum applied to all bogie axles of train by means of dynamic method. The dynamic equation of Straddle-type Monorail train-track system in vertical direction and the four-body model system are established. Comparisons with experimental data, the results suggest that:

1. The dynamic model of monorail train was established for the first time, and the simulation model of monorail train was established based on the dynamic model, which laid the theoretical foundation for the subsequent analysis and research of monorail train dynamics.

2. The effects of DTP, road surface roughness and finger band on train vertical vibration are discussed. Three kinds of excitations are simultaneously added to train model by dynamic method, and dynamic simulation is carried out. That is a new method for dynamic simulation of monorail train is proposed.

3. In time domain diagram, the vertical vibration of train is obviously lower than the measured value before the DTP added, and after the DTP added, the simulation data have been greatly improved, which shows that the deformation of track beam has a great influence on vehicle vibration in time domain.

4. In the frequency domain diagram, the simulation and test show that the vertical vibration frequency of the front bogie is less than 15Hz. Compared with the measured data, before adding the DTP, the main frequency of the first bogie center vibration of the second car is slightly higher, the bandwidth is larger, and the interference waves near the main frequency are more; after adding the DTP, the main frequency of the first bogie Center vibration of the second car is almost the same as the measured data, the waveforms in low frequency band (less than 6HZ) are similar to the measured ones, and the interference waves within 15Hz are much less.

Reference

1. **Simpson, B. J.** 1993. Urban public transport today. London; New York: Routledge. http://doi.org/10.4324/9780203362235.
2. **Zhong, J. H.** 2013. Structure and Analysis of Turnout for Straddle Type Monorail Traffic Vehicle. China Communications Press.
3. **Reza, N.** Vehicle Dynamics: Theory and Applications. Springer.2008. http://doi.org/ 10.2514/1.46370.
4. **Wen, X. X.; He, Y. T.** 2012. Crash simulation of straddle-type monorail vehicle body and human injury research, Advanced Materials Research 413: 486-490. http:// doi.org/10.4028/www.scientific.net/amr.413.486.
5. **Wen, X. X.; Du, Z. X.** 2015. The application of genetic algorithm on the traction speed curve optimizing of the monorail train, Journal of Information and Computational Science 12(15): 5835-5846.
6. **Du, Z. X.** 2017. Numerical analysis of partial abrasion of the straddle-type monorail vehicle running tyre, Transactions of Famena 41(1): 99-112. http://doi.org/ 10.21278/TOF.41109.
7. **Zhou, J. C.; Du, Z. X.** 2019. Dynamic response of the full-scale straddle-type monorail vehicles with single-axle bogies, Mechanika 25(1): 17-24.
8. **Wen, X. X.; Du, Z. X.** 2017. The coupling dynamic model and vibration response of straddle type monorail vehicle. journal of vibration, Measurement and Diagnosis 37(3): 462-468.
9. **Zhou, J. C.; Du, Z. X.** 2019. Dynamic parameters optimization of straddle-type monorail vehicles based multiobjective collaborative optimization algorithm, Vehicle System Dynamics. http://doi.org/10.1080/00423114.2019.1578384.
10. **Zhou, J. C.; Du, Z. X.** 2018. An optimization design of vehicle axle system based on multi objective cooperative optimization algorithm, Journal of the Chinese Institute of Engineers 41(8):635-642. http://doi.org/10.1080/02533839.2018.1534559.
11. **Meysam, Naeimi.** 2015. Dynamic interaction of the monorail–bridge system using a combined finite element multibody-based model, Journal of Multi-body dynamics 229(2): 132-151. http://doi.org/10.1177/1464419314551189.
12. **Lv, KK.** 2017. Influence of wheel eccentricity on vertical vibration of suspended monorail vehicle: experiment and simulation, Shock and Vibration 1367683. http://doi.org/ 10.1155/2017/1367683.
13. **Kim, C. W.** 2013. Seismic behavior of steel monorail bridges under train load during strong earthquakes, Journal of Earthquake and Tsunami 7(2): 1350006. http://doi.org/10.1142/S1793431113500061.
14. **Pu, Q. H.** 2018. Fatigue behavior of prestressed concrete beam for straddle-type monorail tracks, Applied Sciences-Basel 8(7): 1136. http://doi.org/ 10.3390/app8071136.
15. **Hongye, Gou.** 2018. Dynamic response of a long-span concrete-filled steel tube tied arch bridge and the riding comfort of monorail trains, Applied Sciences-Basel 8(4): 650. http://doi.org/10.3390/app8040650.
16. **Bao, Y. L.** 2016. A case study of dynamic response analysis and safety assessment for a suspended monorail system, International Journal of Environmental Research and Public Health 13(11): 1121. http://doi.org/10.3390/ijerph13111121.
17. **Zhouzhou, X.** 2017. Research on vertical coupling dynamics of monorail vehicle at finger-band, Urban Rail Transit. http://doi.org/10.1007/s40864-017-0065-1.

Zhouzhou Xu, Zixue Du, Zhen Yang, Junchao Zhou

RESEARCH ON VEHICLE-BRIDGE VERTICAL COUPLING DYNAMICS OF MONORAIL BASED ON MULTIPLE ROAD EXCITATIONS

S u m m a r y

In order to study the vertical dynamic behavior of the monorail-bridge system, the vehicle-bridge coupling dynamic equation and train simulation model are established based on the principle of dynamics; the train simulation model is established based on the multi-body dynamics; the track model is established based on the finite element theory, and the compression deformation of PC beam and the effect of finger band on train are equivalent to load spectrum on train axle by means of dynamic equivalence principle, and finally, the train-track interaction model is established; the vertical vibration of the train before and after adding the influence of the compressive deformation of the track beam is simulated and calculated respectively, the results show that the influence of the compressive deformation of the track beam on the vertical vibration of the train is significant, and the simulation data under multiple road excitations are very close to the real value.

Keywords: monorail, vehicle-bridge coupling dynamics, road excitation, deformation of track beam caused by pressure.

Received October 11, 2019
Accepted August 24, 2020